

Cathodoluminescence and microRaman analysis of oxygen loss in electron irradiated $\text{YBa}_2\text{Cu}_3\text{O}_{7-x}$

P. Gómez^{a)}

Departamento de Física de Física de Materiales, Facultad de Física, Universidad Complutense, 28040-Madrid, Spain and Departamento de Física Aplicada, E.U.I.T.A., Universidad de Castilla-La Mancha, 13071-Ciudad Real, Spain

J. Jiménez and P. Martín

Departamento de Física de la Materia Condensada, ETS Ingenieros Industriales, 47011-Valladolid, Spain

J. Piqueras and F. Domínguez-Adame

Departamento de Física de Materiales, Facultad de Física, Universidad Complutense, 28040-Madrid, Spain

(Received 9 April 1993; accepted for publication 16 July 1993)

The effect of oxygen loss on the luminescence of $\text{YBa}_2\text{Cu}_3\text{O}_{7-x}$ has been investigated by cathodoluminescence (CL) in the scanning electron microscope (SEM) and by Raman microprobe measurements. The results herein indicate that a CL band at 530 nm is related to oxygen loss rather than to impurity phases such as Y_2O_3 formed in the material by electron irradiation in the SEM.

I. INTRODUCTION

Cathodoluminescence (CL) signal of $\text{YBa}_2\text{Cu}_3\text{O}_{7-x}$ (YBCO) increases during electron irradiation in the scanning electron microscope.^{1,2} The evolution of the CL intensity and spectra under an electron beam has been described elsewhere.² This effect, which enables one to generate localized luminescent regions in YBCO, has been attributed to structural changes caused by electron-induced oxygen loss. In the present work this possibility is further investigated. For this purpose the oxygen content in electron irradiated regions of YBCO has been compared with that in unirradiated regions by means of microRaman measurements and the CL emission in the same samples has been measured. On the other hand, the CL behavior of the samples irradiated in the electron microscope has been compared with that of samples undergoing other treatments causing oxygen loss, such as laser irradiation or vacuum annealing.

II. EXPERIMENTAL METHOD

The samples were sintered $\text{YBa}_2\text{Cu}_3\text{O}_{7-x}$ with nominal T_c values of 93 K. Well-defined regions of a sample were electron irradiated at 30 keV in the scanning electron microscope (SEM) by performing a repetitive scan line. The irradiated line was identified in the emissive mode image by the appearance of a rough surface in a region about 10 μm wide.

MicroRaman measurements were performed at different points along a line perpendicular to the irradiated line. The excitation was done with the 514.5 nm line of an Ar^+ laser through a 100 \times microscope objective with a large numerical aperture ($\text{NA}=0.950$). The laser spot at the focal plane had a diameter smaller than 1 μm , which is the lateral resolution of the Raman microprobe. Both the excitation and the light collection were done through the microscope objective, hence the measurement geometry was backscattering. The Raman spectrometer was a

DILOR XY equipped with multichannel detection. The laser power density was low enough to avoid local heating that might damage the sample. The sample was mounted on a motorized X-Y stage that allows high precision regularly spaced point by point Raman measurements. All measurements were carried out at room temperature and no special preparation of the sample was required.

Other samples were annealed at 10^{-2} Torr at temperatures between 100 and 500 $^\circ\text{C}$ for 20 h or irradiated at 10^{-2} Torr with a multiwavelength Ar ion laser. Luminescence of treated and untreated samples was measured in the SEM with a previously described experimental arrangement.³

III. RESULTS AND DISCUSSION

In general, untreated samples show a low CL emission that becomes readily detectable after a certain observation time in the SEM due to electron irradiation. For this reason CL spectra of nominally untreated samples are often modified by the electron irradiation. However, spectra recorded at the first stage of observation indicate that the CL emission of untreated samples is mainly related to a band in the 400–450 nm region. This agrees with the observation of Stankevich *et al.*⁴ that a band at 440 nm is inherent to $\text{YBa}_2\text{Cu}_3\text{O}_{7-x}$ crystals. Figure 1 shows the CL image of the electron irradiated line and Fig. 2 the corresponding CL spectrum of this region. The spectrum shows a band in the 500–550 nm spectral range previously associated to electron beam effects. The width of the luminescent region is not constant along the line and ranges between 15 and about 20 μm .

Figure 3 shows the Raman spectra obtained at different points along a line crossing the electron irradiated region. An optical microscopy (Nomarsky) inspection reveals a highly damaged region ($\sim 10 \mu\text{m}$ wide), surrounded by a slightly damaged region, which extends about 10–15 μm out of the damaged region. These areas

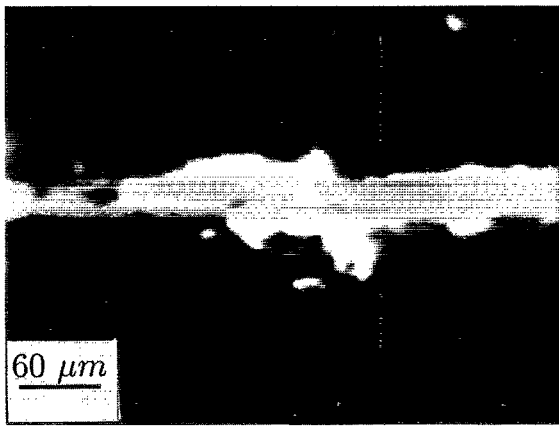


FIG. 1. CL image from an electron irradiated line.

correspond to those seen by CL imaging and will be henceforth labeled as undamaged region, slightly damaged region and heavily damaged region respectively.

The spectrum obtained in the undamaged region is according to the Raman scattering selection rules typical of the $c||$ oriented crystals, which give a spectrum characterized by a strong peak at $\sim 500 \text{ cm}^{-1}$, associated to the stretching of the bridging oxygen.⁵ The peak at 335 cm^{-1} is practically unobservable in this scattering configuration and is associated with in-plane CuO_2 oxygen vibrations out of phase.⁵ The frequency shift of the 500 cm^{-1} peak allows the oxygen content of the $\text{YBa}_2\text{Cu}_3\text{O}_{7-x}$ crystals to be assessed.⁶⁻⁸ As the region surrounding the electron irradiated area, previously identified as the slightly damaged region, is probed by the laser beam a downward frequency shift of the 500 cm^{-1} peak is observed; together with this frequency softening an increase of the $I(335)/I(500)$ intensity ratio is seen. All that provides clear evidence of the oxygen decrease in this slightly damaged region.^{6,7} Figure 4 shows the frequency shift of the 500 cm^{-1} peak as a function of the position along the scanning line.

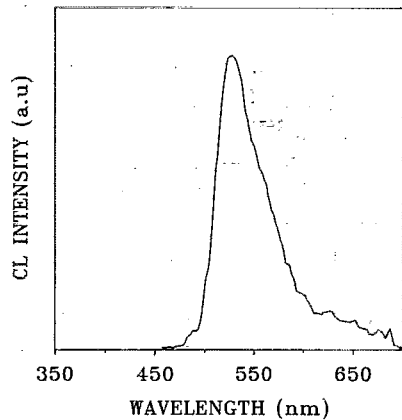


FIG. 2. CL spectrum from the same electron irradiated line shown in Fig. 1.

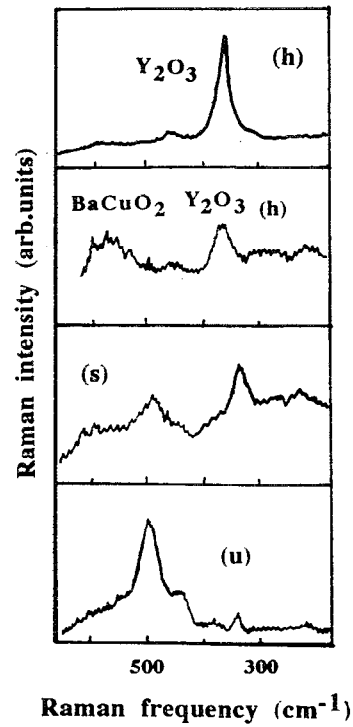


FIG. 3. Raman spectra obtained at different points of the undamaged region (u), slightly damaged region (s), and heavily damaged region (h).

When the laser beam probes the heavily damaged region the Raman spectrum becomes very noisy, showing a strong oxygen loss (large x) and the local formation of impurity phases, mainly oxides, at different points of the irradiated area. The frequency shift of the 335 cm^{-1} peak is shown as a function of position in Fig. 5; in both the undamaged and the slightly damaged regions it corresponds to $\text{YBa}_2\text{Cu}_3\text{O}_{7-x}$ with different oxygen content. Raman spectroscopy can be used to determine the oxygen content of YBCO. In fact, the frequency of the 500 cm^{-1} Raman peak is strongly sensitive to the oxygen content; it

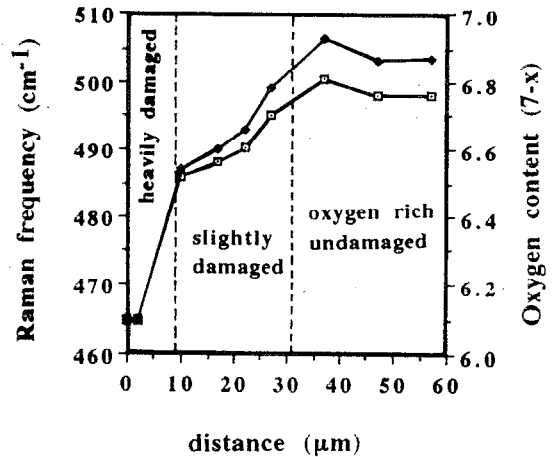


FIG. 4. Frequency of the 500 cm^{-1} Raman band across the scanning line. Oxygen content estimated from the frequency shift of the 500 cm^{-1} Raman peak.

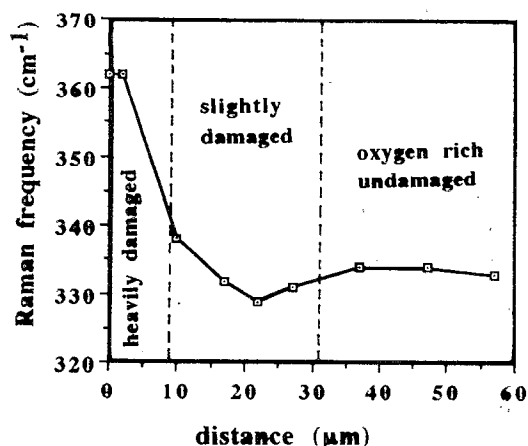


FIG. 5. Frequency of the 335 cm^{-1} Raman band across the scanning line. Inside the heavily damaged region appear at localized points the Y_2O_3 related band.

is downward shifted as the oxygen concentration is depressed. Thus, Raman spectroscopy is an established, non-destructive tool for determining the oxygen composition in YBCO. The estimated oxygen content is plotted as a function of the distance along the scanning line in Fig. 4 according to the following relationship⁸

$$x = 0.027\nu(500) - 6.58.$$

Inside the heavily damaged region this peak is significantly shifted to the blue. Such a shift cannot be accounted for by the disorder induced by the electron irradiation in the YBCO lattice; disorder could activate vibration modes which are initially Raman forbidden, nevertheless no infrared modes are seen in YBCO in this frequency range.⁹ On the other hand, for extreme oxygen loss the frequency shift reported for the 335 cm^{-1} peak is much smaller than that measured herein.⁷ For this reason, the 360 cm^{-1} peak measured at local points of the damaged region is probably associated with the formation of the Y_2O_3 impurity phase, which presents a similar Raman spectrum with a strong peak at this frequency.¹⁰ The formation of impurity phases in localized points of this region is confirmed by the identification of the BaCuO_2 phase, which is identified through the Raman peaks at 575 and 640 cm^{-1} .¹¹ It should be noted that the Raman cross section of these phases is much larger than the Raman cross section for the YBCO,¹¹ therefore, no big quantities of these phases are expected from the Raman intensity measured. Anyway, the observation of these phases is not regular along the heavily damaged region, but it is rather localized at particular points. The presence of impurity phases in high T_c YBCO is usually reported to occur at the intergrain regions,¹¹ the most generally observed phases due to the sintering procedure are the green phase, Y_2CuO_5 and BaCuO_2 . No Y_2O_3 was observed in the many examined samples, both thin films or ceramics, out of the damaged area. The formation of impurity phases as a result of different treatments is usually observed, i.e., laser ablation¹² and ion irradiation.¹³ The results we present herein support the formation of these

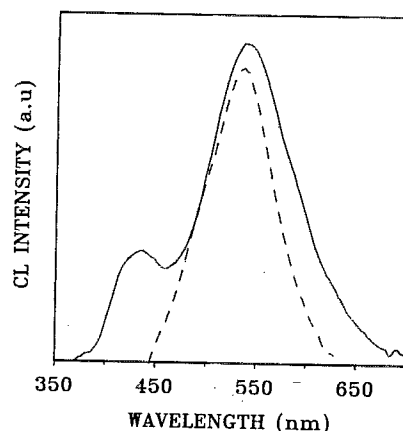


FIG. 6. CL spectra from samples after weak (solid line) and strong (dashed line) treatments.

phases by electron irradiation as well. The fact that these phases are observed at localized point of the irradiated area could be associated with a gettering at special points, probably intergrains, where the temperature during irradiation is expected to be significantly enhanced.

The present Raman microprobe measurements reveal oxygen loss and the formation of impurity phases at localized points. This is consistent with CL measurements that associate the light emission at 530 nm with oxygen depletion rather than with Y_2O_3 which could account for local CL emission. Y_2O_3 is characterized by a strong 365 nm luminescence emission at low temperature^{14,15} which is not seen in our measurements. In order to get insight about this point we are doing similar measurements in samples prepared with different oxygen content without electron irradiation.

Similar to electron irradiation, laser irradiation produces a rough surface and enhanced CL emission in the irradiated area. Laser irradiation as well as annealing treatments cause different CL spectra that can be qualitatively represented by the spectra of Fig. 6. After short laser irradiation or low- (200°C) temperature annealing the spectrum shown by the solid line is obtained while longer irradiation times or higher- (400°C) temperature annealing produce the spectrum shown by the dashed line. It appears that all treatments cause the appearance of a luminescence band at 530 nm . After moderate treatments the intrinsic 440 nm emission is still detectable but after more severe treatments the increase of the 530 nm emission mask the 440 nm band. This result shows that laser irradiation or vacuum annealing have similar effect on luminescence from $\text{YBa}_2\text{Cu}_3\text{O}_{7-x}$ to that of the electron irradiation. The annealing and laser irradiation treatments undergone by our samples are known^{16,17} to produce oxygen depletion. This indicates that the 530 nm CL emission is associated with oxygen depleted zones, but cannot be associated, with the available data, to specific defects in the material.

Since CL appears to be sensitive to structural changes in $\text{YBa}_2\text{Cu}_3\text{O}_{7-x}$, the dependence of CL intensity on temperature could in some cases be used to detect specific

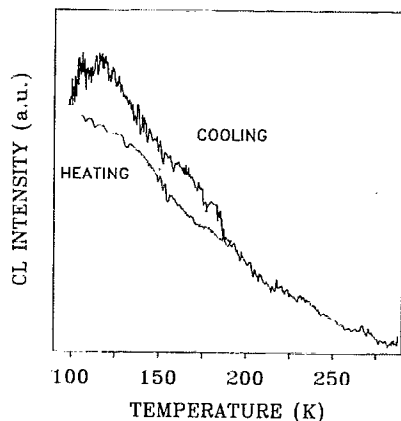


FIG. 7. Temperature dependence of CL intensity in a sample after laser irradiation treatment.

changes. This possibility, supported by previous results on high-temperature superconductor films,¹⁸ has also been studied in this work. Figure 7 shows the temperature dependence of CL intensity in a sample after laser irradiation treatment. A hysteretic behavior in heating and cooling runs has been observed by several authors in the measurements of acoustic properties of YBCO¹⁹⁻²¹ and has been sometimes attributed to fine structural transitions involving reordering of oxygen atoms or vacancies. It is suggested that CL evolution could reflect some of these changes.

IV. CONCLUSIONS

Electron irradiation in the SEM causes the appearance of a CL emission band at about 530 nm. Raman microprobe measurements reveal oxygen loss and formation of impurity phases, such as Y₂O₃ and BaCuO₂, at localized points. These observations indicate that the mentioned CL emission is associated with oxygen depletion rather than with the presence of an extended Y₂O₃ dielectric phase.

ACKNOWLEDGMENTS

This work was partially supported by DGICYT (Project PB 90-1017). The help of Dr. J. A. García and Dr. A. Remón is acknowledged.

- ¹J. H. Miller, D. J. Hunn, S. L. Holder, and A. N. DiBianca, *Appl. Phys. Lett.* **56**, 89 (1990).
- ²J. Piqueras, P. Fernández, and J. L. Vicent, *Appl. Phys. Lett.* **57**, 2722 (1990).
- ³B. Méndez and J. Piqueras, *J. Appl. Phys.* **69**, 2776 (1991).
- ⁴V. G. Stankevich, N. Yu. Svechnikov, K. V. Kaznacheev, R. A. Kink, I. L. Kuusmann, É. Kh. Feldbach, G. Zimmerer, T. Kloiber, A. A. Zhokhov, G. A. Emel'chenko, M. A. Kalyagin, and V. Ya. Kosyev, *J. Lumin.* **48/49**, 845 (1991).
- ⁵C. Thomsen, M. Cardona, and R. Liu, *J. Less Common Metals* **150**, 33 (1989).
- ⁶G. Burns, F. H. Dacol, and F. Holtzberg, *Solid State Commun.* **75**, 893 (1990).
- ⁷G. Burns, F. H. Dacol, and F. Holtzberg, *Solid State Commun.* **77**, 367 (1991).
- ⁸Phan V. Huong, J. C. Bruyère, E. Bustarret, and P. Grandchamp, *Solid State Commun.* **72**, 191 (1989).
- ⁹J. Chrzanowski, S. Gygax, J. C. Irvin, and W. N. Hardy, *Solid State Commun.* **65**, 139 (1988).
- ¹⁰R. Bhadra, T. O. Brun, M. A. Beno, B. Dabrowski, D. G. Hinks, J. Z. Liu, J. D. Jorgensen, L. J. Nowicki, A. P. Paulickas, I. K. Schuller, C. U. Segre, L. Soderholm, B. Veal, H. H. Wang, J. M. Williams, K. Zhang, and M. Grimsditch, *Phys. Rev. B* **37**, 5142 (1988).
- ¹¹A. Erle, S. Blumenroder, E. Zirngielb, and G. Guntherodt, *Solid State Commun.* **73**, 753 (1990).
- ¹²J. Jiménez (unpublished).
- ¹³M. V. Belousov, F. A. Chudnovskii, V. Y. Davidov, B. S. Elkin, S. L. Shokhor, and V. Y. Velichko, *Solid State Commun.* **81**, 493 (1992).
- ¹⁴W. Hayes, M. J. Kane, O. Salminen, and A. I. Kuznetsov, *J. Phys. C* **17**, L383 (1984).
- ¹⁵V. V. Mürk, A. I. Kuznetsov, and B. R. Namozov, *Phys. Status Solidi A* **63**, K131 (1981).
- ¹⁶S. Matsui, T. Ichihashi, T. Yoshitake, S. Miura, T. Satoh, and M. Mito, *J. Vac. Sci. Technol. B* **8**, 1771 (1990).
- ¹⁷Y. Q. Shen, T. Freltoft, and P. Vase, *Appl. Phys. Lett.* **59**, 1365 (1991).
- ¹⁸F. Domínguez-Adame, P. Fernández, J. Piqueras, P. Prieto, C. Barrero, and M. E. Gómez, *J. Appl. Phys.* **71**, 2778 (1992).
- ¹⁹V. Müller, C. Hucho, K. de Groot, D. Winau, D. Maurer, and K. H. Rieder, *Solid State Commun.* **72**, 997 (1989).
- ²⁰O. Yu. Sersobol'skaya, S. P. Tokmakova, and L. A. Chernozatonskii, *Sov. Phys. Solid State* **33**, 1209 (1991).
- ²¹L. N. Pal-val, P. P. Pal-val, V. D. Natsik, and V. I. Dotsenko, *Solid State Commun.* **81**, 761 (1992).